Experimental Mechanics (2009) 49:125–134
DOI 10.1007/s11340-008-9143-3

Morphological Responses of Vascular Endothelial Cells Induced by Local Stretch Transmitted Through Intercellular Junctions

Y. Ueki · N. Sakamoto · T. Ohashi · M. Sato

Received: 6 June 2007 / Accepted: 24 March 2008 / Published online: 23 April 2008

Abstract It has been well established that mechanical stimuli including fluid shear stress and cyclic stretch play a key role in endothelial cell (EC) remodeling. However, in contrast to global remodeling to these mechanical stimuli, little is known of how local mechanical forces are transmitted through cells to induce cell remodeling leading to alteration in cell functions. In this study, we demonstrated that EC remodeling can be exerted by local tension generated in a neighboring EC. In this technique, a glass microneedle was used to apply local stretch in an EC in confluent monolayer and the resulting tension is transmitted to a neighboring EC across intercellular junctions. Local stretch induced reorientation and elongation of ECs parallel to the direction of stretch associated with reorganization of stress fibers. In addition, recruitment of Src homology 2-containing tyrosine phosphatase-2, binding to intercellular adhesion molecules platelet-endothelial cellular adhesion molecules-1, was selectively observed at the force-transmitted intercellular junctions after application of local stretch. These findings suggest that intercellular junctions can not only transmit but also sense local forces, and are potentially involved in EC mechanotransduction pathways.

Keywords Endothelial cell remodeling · Stress fibers · Mechanotransduction · Intercellular junction · Adhesion molecules

Y. Ueki (✉) · N. Sakamoto · T. Ohashi · M. Sato
Department of Bioengineering and Robotics,
Graduate School of Engineering, Tohoku University,
6-6-01 Aramaki-aoba,
Sendai 980-8579, Japan
e-mail: ueki@bml.mech.tohoku.ac.jp

N. Sakamoto
e-mail: naoya@bml.mech.tohoku.ac.jp

T. Ohashi
e-mail: ohashi@bml.mech.tohoku.ac.jp

M. Sato
Department of Biomedical Engineering,
Graduate School of Biomedical Engineering, Tohoku University,
6-6-01 Aramaki-aoba,
Sendai 980-8579, Japan
e-mail: sato@bml.mech.tohoku.ac.jp

Introduction

Endothelial cells (ECs) lining inner surfaces of blood vessels are exposed to a variety of mechanical stimuli including fluid shear stress due to blood flow, cyclic stretch due to the wall deformation, and hydrostatic pressure due to blood pressure. Since the relationship between EC morphology and mechanical conditions has been implicated in vascular pathology such as atherosclerosis, in vitro model systems have been widely used to investigate the effects of mechanical stimuli on EC remodeling. Most previous studies have exclusively applied global mechanical stimuli including fluid shear stress [1–4], cyclic stretch [5, 6] and hydrostatic pressure [7, 8] to cultured EC monolayer. For example, under exposure to fluid shear stress, ECs exhibit elongation and alignment parallel to the direction of flow concomitant with reorganization of actin stress fibers (SFs) [2, 4]. It is also well known that ECs exposed to cyclic stretch elongate and align perpendicular to the direction of stretch [5]. Furthermore, pressure-imposed ECs elongate with random orientation [7]. Thus, ECs respond very specifically to the type of mechanical stimuli, raising the question of how externally applied mechanical forces transmit in cells and where the transmitted forces are sensed and converted into biochemical signals. It has been suggested that mechanotransduction of ECs may occur at

specific sites located in cell membrane (e.g. stretch activated channels (SACs)), attachment points of ECs to extracellular matrix (e.g. integrins), intercellular junctions (e.g. platelet-endothelial cellular adhesion molecules-1, PECAM-1) and more likely a combination of these sites. However, the details of these mechanotransducers in cell signaling pathways remain unclear, because, in part, there is a possibility that these mechanotransducers can be simultaneously activated by the globally applied mechanical stimuli. Therefore, it is necessary to develop an experimental method, with which each mechanotransducer can be selectively stimulated.

Intercellular junctions of ECs involve adherens-junctions, tight-junctions, gap-junctions and PECAM-1 junctions. Particularly, adherens-junctions composed of VE-cadherin which is connected to actin-cytoskeleton via α/β catenins are thought to exclusively mediate forces at intercellular junctions by forming homophilic binding, probably because mechanical coupling by adherens-junctions may be stiffer than the other junctions. Recently, there has been a growing attention on the role of intercellular adhesion molecules with implications of EC mechanotransduction signalling pathways. PECAM-1 is known to form homophilic binding between neighboring ECs [9] in the vicinity of adherens-junctions and be connected to actin-cytoskeletons via β/γ catenins [10]. Previous reports revealed that ECs under sparse conditions do not show morphological changes in response to fluid shear stress [11, 12]. Osawa et al. [13] reported that PECAM-1 is rapidly tyrosine-phosphorylated when ECs are exposed to fluid shear stress or hyper osmotic shock, and bind to a protein tyrosine phosphatase Src homology 2-containing tyrosine phosphatase-2 (SHP-2) to activate intracellular signal cascades. Tzima et al. [14] reported that PECAM-1-mediated mechanotransduction is involved in the upstream of the integrin signaling cascade, leading to cytoskeletal reorganization in flow conditioned ECs. This leads to an idea that transmitted forces at adherens-junctions may stimulate PECAM-1 phosphorylation, leading to SHP-2 activation followed by morphological changes of ECs. Thus, PECAM-1 may be responsible for morphological responses to mechanical stimuli transmitted through intercellular junctions serving as one of principal mechanotransducers.

To test this hypothesis, in this study, local stretch was applied to an EC by using a microneedle to selectively stimulate intercellular junctions between the EC and a neighboring EC. After application of mechanical stimuli, morphological changes of the neighboring EC were fluorescently observed to test the hypothesis that local stimuli are transmitted via intercellular junctions and induce EC remodeling. In addition, localization of SHP-2 was observed to assess whether PECAM-1 is involved in the mechanotransduction pathways.

Materials and Methods

Cell Culture and Transfection

Human umbilical vein endothelial cells (HUVECs) were obtained from umbilical veins with trypsin treatment adapted from Sakamoto et al. [15]. Cells were cultured in Medium 199 (Invitrogen, USA) containing 20% fetal bovine serum (Sigma-Aldrich, USA), 10 ng/ml basic fibroblast growth factor (Austral Biologicals, USA) and penicillin–streptomycin (Invitrogen), and were used from the third to the sixth passage. For experiments, cells were plated on a glass base culture dish (ø=35 mm, Asahi Techno Glass, Japan) coated with 0.1% gelatin (Sigma-Aldrich). A plasmid encoding enhanced green fluorescent protein (EGFP)-actin (Clontech, USA) was transfected into HUVECs with a liposomal method using Lipofectin (Invitrogen) according to the manufacturer's protocol for visualization of actin cytoskeleton.

Local Stretch Experiment

Figure 1 shows the experimental setup used to apply local stretch. A glass microneedle with a diameter of ca. 1 μm

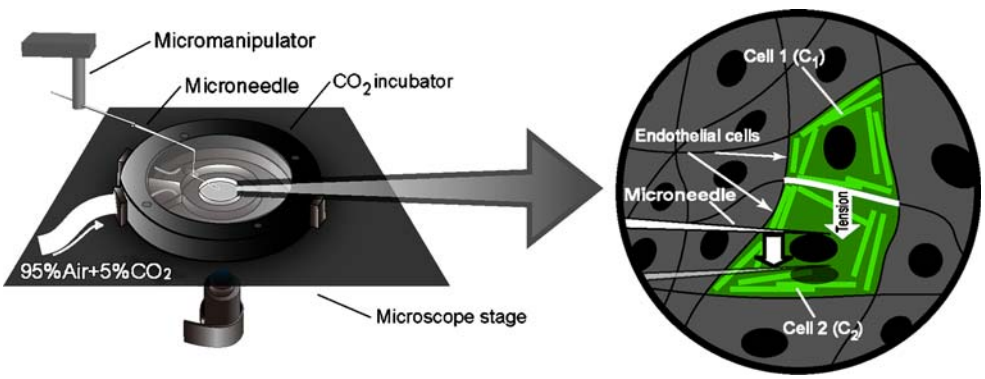

Fig. 1 Schematic illustrations of experimental system for local stretch application. A microneedle was used to apply local stretch to C_2, possibly inducing remodeling of C_1 via intercellular junctions. The experiments were performed in a CO_2 incubator at 37°C and 5% CO_2

was made from a glass tube (ø=1 mm, GD-1, Narishige, Japan) using a pipette puller (PP-83, Narishige, Japan) and manipulated by a 3-D hydraulic micromanipulator. A pair of ECs (cell 1 (C_1) and cell 2 (C_2)) in the figure) expressing EGFP-actin were selected under a confocal laser scanning microscope (CLSM, FV1000, Olympus, Japan), and the nucleus of C_2 was then moved horizontally by 10 μm by manipulating the glass microneedle to locally stretch C_1. This procedure allows us to mimic cell deformation induced by externally applied local tension via intercellular junctions between C_1 and C_2. In a separate study, particle tracer velocimetry (PTV) method was performed to calculate distribution of intracellular deformation induced by local stretch by using a software (Flowvec, Library, Japan) (Fig. 2). The result showed that high displacement was observed specifically at the intercellular junctions between C_1 and C_2, confirming force transmission across the junctions. After application of local stretch, fluorescent images were obtained up to 60 min at intervals of 5 min with the CLSM to assess features of C_1 remodeling process. All procedures were performed in a CO_2 incubator (MI-IBC, Olympus) mounted on the microscope stage to maintain the cell culture environment at 37°C and 5% CO_2.

Image Analysis

Image analysis was performed to evaluate morphological and cytoskeletal changes of C_1 using the following parameters: angle of cell orientation, cell aspect ratio, angle of SF orientation and uniformity index of SF. Angle of cell orientation and cell aspect ratio were calculated with the public domain program Image J version 1.37v (National Institute of Health, USA). A cell outline was manually extracted from a fluorescence image of GFP-actin by tracing the cell edge. An equivalent ellipse for the cell outline was automatically determined with a function of the software. An angle between the major axis of the ellipse and the direction of stretch was then defined as the angle of cell orientation. A ratio of length of the minor axis to the major axis was defined as the cell aspect ratio, with being 1.0 for circles and approaching zero for highly elongated shape. Analyses were performed on the fluorescent images obtained at every 5 min after application of local stretch. See Appendix for details of the angle of SF orientation and the uniformity index of SF.

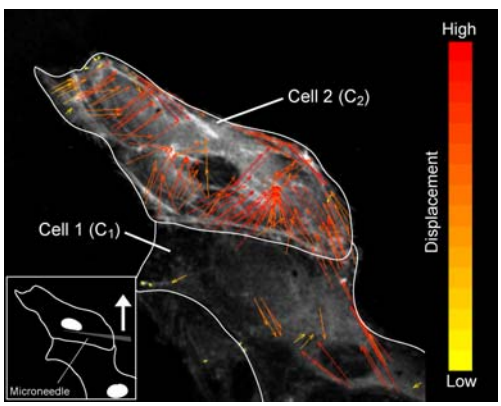

Fig. 2 Distribution of intracellular displacement calculated by using PTV method. Longer arrows represent higher displacement. Applied local stretch in C_2 was found to be transmitted to C_1 at intercellular junctions

SACs Blocking Experiment

In order to inhibit function of SACs, 20 μM $GdCl_3$ (Wako pure chemical, Japan) was added to cell culture medium at 30 min before application of local stretch.

Immunofluorescence

Localization of SHP-2 was examined with immunofluorescence. ECs were pre-incubated with 1 mM $NaVO_3$ (Wako Pure Chemical, Japan) for 30 min to enhance tyrosine phosphorylation before application of local stretch. Five minutes after the mechanical loading, ECs were then fixed in 4% paraformaldehyde (Wako Pure Chemical) containing 1 mM $NaVO_3$ for 15 min at 4°C. Next, ECs were permeabilized with 0.1% Triton X (Wako Pure Chemical), blocked with Block ace (Dainippon Sumitomo Pharma, Japan), and stained with anti-SHP-2 mouse monoclonal antibody (Santa Cruz Biotechnology, USA) and Alexa fluor 594 anti-mouse IgG (Invitrogen).

Statistical Analysis

Statistical comparisons in morphological parameters were performed using repeated measures analysis of variance (ANOVA) followed by Bonferroni's multiple comparison (0 min vs 30 min, 60 min). A p value less than 0.05 was considered as significant. Data are expressed a mean± SEM.

Results

Morphological Changes of ECs After Application of Local Stretch

Typical florescent images of EGFP-actin were shown in Fig. 3 at 0 min, 30 min and 60 min after application of local stretch. The observed cell C_1 initially elongated perpendicular to the direction of stretch [Fig. 3(a)] exhibited contraction at 30 min [Fig. 3(b)] followed by elongation

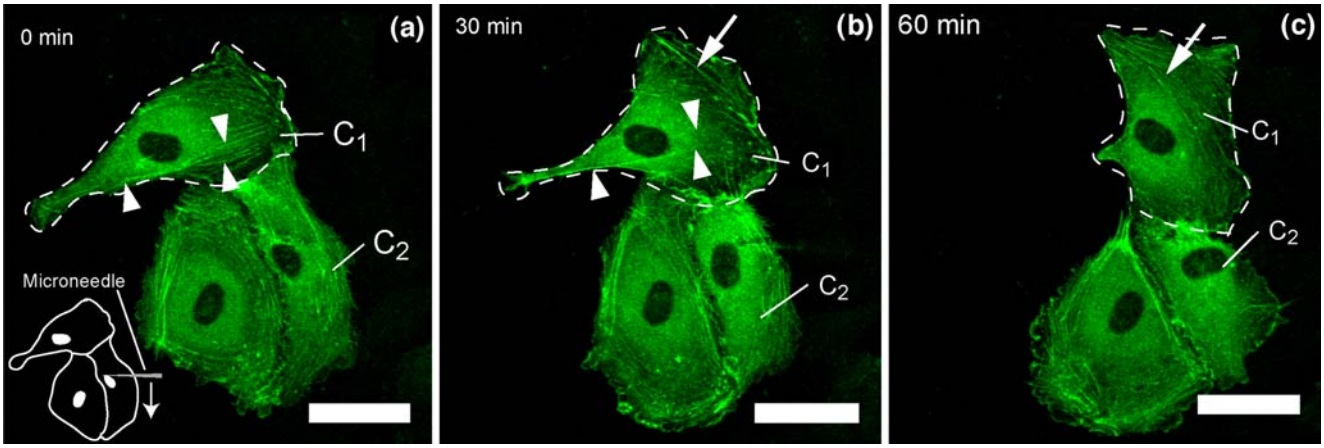

Fig. 3 Typical examples of fluorescent images of EGFP-actin at (**a**) 0 min, (**b**) 30 min, and (**c**) 60 min after application of local stretch. Broken lines indicate the edge of C_1. The horizontally elongated C_1 at 0 min (**a**) showed contraction at 30 min (**b**) and re-elongated parallel to the direction of the stretch at 60 min (**c**). Preexisting SFs at 0 min (**a**) disappeared at 30 min (**b**) and new SFs formation was observed at 60 min (**c**). Bar=40 μm

parallel to the direction of stretch at 60 min [Fig. 3(c)]. Concurrently with these morphological changes, SFs initially orientated perpendicular to the direction of stretch at 0 min [Fig. 3(a), arrowheads], and disappeared [Fig. 3(b), arrowheads] while formation of new SFs parallel to the direction of stretch was observed [Fig. 3(b), arrow] at 30 min. The new SF formation was continuously observed at 60 min [Fig. 3(c), arrow].

Figure 4 represents distribution of the angle of cell orientation and the cell aspect ratio of the observed cell C_1 at 0 min, 30 min and 60 min. From different types of initial cell morphology, the experimented data can be divided into two groups: Group A, ECs with angle of cell orientation >60° and aspect ratio <0.5; Group B, the rest of Group A. Roughly, distribution of the two groups is schematically drawn in the figure by ellipsoids. For both Groups, the angle of cell orientation significantly decreased from 0 min [Fig. 4(a), 71.3±4.4°, 53.3±4.6° for Groups A and B, respectively] to 60 min [Fig. 4(c), 52.1±6.8°, and 29.0±3.7° for Groups A and B respectively, $p<0.05$ vs 0 min for both groups]. For Group A, aspect ratio significantly increased from 0 min [Fig. 4(a), 0.42±0.02] to 30 min [Fig. 4(b), 0.57±0.07, $p<0.05$ vs 0 min] and then decreased at 60 min [Fig. 4(c), 0.53±0.08, NS vs 0 min]. On the other hand, for Group B, aspect ratio did not show a significant change from 0 min [Fig. 4(a), 0.57±0.05] to 30 min [Fig. 4(b), 0.55±0.07] and significantly decreased at 60 min [Fig. 4(c), 0.47±0.06, $p<0.05$ vs 0 min].

Time course of change in the SF parameters is summarized in Fig. 5. Angle of SF orientation for both groups significantly decreased at 60 min [Fig. 5(a), $p<0.05$, vs 0 min]. For Group A, change in the uniformity index was not significant between 0 min and 60 min [Fig. 5(b)] while the uniformity index significantly increased at 60 min for Group B [Fig. 5(b), $p<0.05$ vs 0 min].

SACs Blocking Experiment

SACs blocking experiment was performed on Group B with treatment of $GdCl_3$. Treated cells showed the similar time course of change in morphology, and morphological parameters showed no significant difference compared to those of non-treated control cells (data not shown). This result indicates that SACs should not be involved in the present remodeling.

Change in Distribution of SHP-2 After Application of Local Stretch

Figure 6 represents typical fluorescent images of EGFP-actin and anti-SHP-2 for control [Fig. 6(a,b,c)] and $GdCl_3$-treated ECs [Fig. 6(d,e,f)] after application of local stretch. For control ECs, recruitment of SHP-2 was clearly observed at the intercellular junctions between C_1 and C_2 [Fig. 6(b,c)]. For $GdCl_3$ -treated ECs, localization of SHP-2 was still observed at the intercellular junctions, suggesting that applied mechanical loading can be transduced into molecular signals [Fig. 6(e,f)].

Discussion

In this study, local tension transmitted via intercellular junctions was applied to ECs to induce morphological changes in a neighboring EC. The result showed that ECs elongate and orient parallel to the direction of stretch

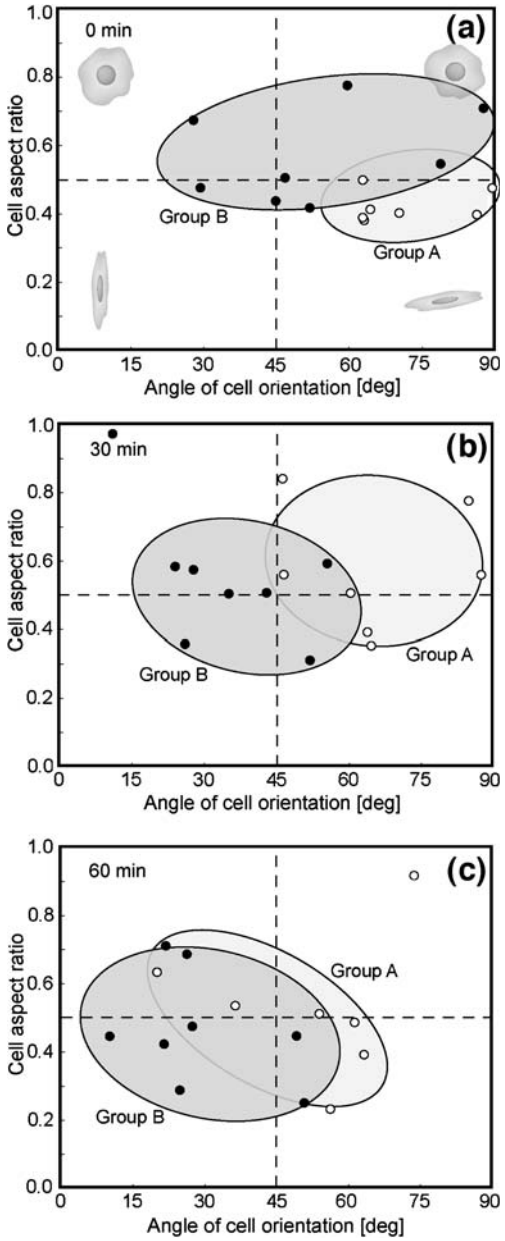

Fig. 4 Changes in morphological parameters of ECs at (**a**) 0 min, (**b**) 30 min and (**c**) 60 min after application of local stretch. Group A represents cells with angle of cell orientation >60° and aspect ratio <0.5 and Group B, the rest of Group A. The two groups showed different time course of changes in the morphological parameters

together with reorganization of stress fibers. Moreover, localization of SHP-2 was selectively observed at intercellular junctions, indicating that mechanotransduction might occur. Most previous studies relating to cell remodeling have utilized global mechanical stimuli including fluid shear stress [1–4] and cyclic stretch [5, 6]. With these conventional techniques, it is difficult to find both mechanotransmission pathways and mechanotransduction sites, probably because these events may occur by a combination of several candidate sensors. To overcome this difficulty, this study proposed a new experimental method to locally apply mechanical stimuli to ECs to identify the role of intercellular junctions involved in EC remodeling.

Interestingly, ECs finally aligned to the direction of stretch at 60 min after application of mechanical stimuli. The mechanism in the present EC remodeling process is unclear. It is well known that ECs exposed to cyclic stretch show alignment perpendicular to the direction of stretch [5]. Sokabe et al. [16] have suggested that when cells are subjected to cyclic stretch, actin cytoskeletons are disassembled during relaxation phase and disruption of actin fibers activates several downstream signals, leading to a cell shape change. On the other hand, ECs under continuous stretch have been shown to align parallel to the direction of stretch [17]. This is consistent with our results in which ECs align to the direction of local continuous stretch, strongly suggesting a critical role of relaxation phase in the EC alignment in response to the two different types of stretch. It is interesting to note that flow-imposed ECs are well known to show alignment to the direction of flow [1, 2, 4]. Although the types of mechanical loadings are different, this tendency is similar to the result of this study in terms of the directional alignment. Several numerical studies have well explained these phenomena of ECs in from the viewpoint of structural optimization. For example, Ohashi et al. [18] reported that ECs exposed to fluid shear stress change their morphology to reduce intracellular stress concentrations. Relating to biomolecular events, Tzima et al. [19] reported that, in ECs exposed to fluid shear stress, Rac1, which is small GTPase controls lamellipodia formation, is locally activated in the downstream region. Likewise, it is worth doing these numerical and extra experimental approaches to elucidate underlying mechanism in the present EC remodeling process. Further investigations may, therefore, include more detailed quantification of intracellular strain field and observations of local activity of Rho small GTPases including Rac1 responsible for reorganization for actin-cytoskeletons.

Time course of change in EC morphology was investigated to characterize EC remodeling process. The remodeling process depended on initial shapes of ECs and thus divided into the two groups: Group A and B. For Group A, ECs initially elongated perpendicular to the direction of stretch exhibited spontaneous contraction prior to elongation/alignment to the direction of stretch. In contrast, for Group B, ECs initially aligned to the direction of stretch immediately exhibited elongation parallel to the direction of stretch. It has been reported that ECs exposed to shear stress show the following time course of change: 1) contraction, 2) reorientation and 3) elongation [7]. Taken

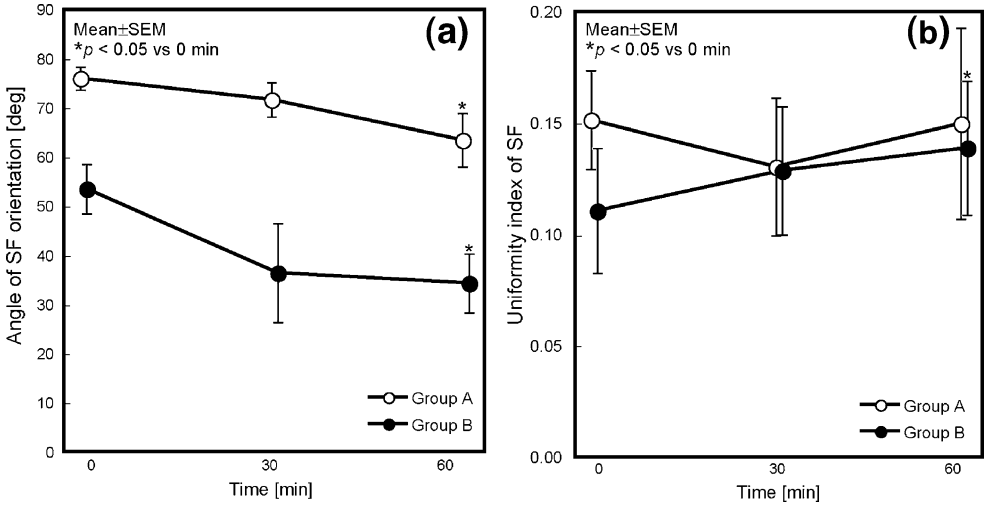

Fig. 5 Time course of changes in SF parameters. (**a**) Angle of SF orientation significantly decreased for both groups. (**b**) Change in uniformity index of SF was not significant for Group A, while the index significantly increased for Group B. See Appendix for details for determination of SF parameters. *p<0.05 vs 0 min

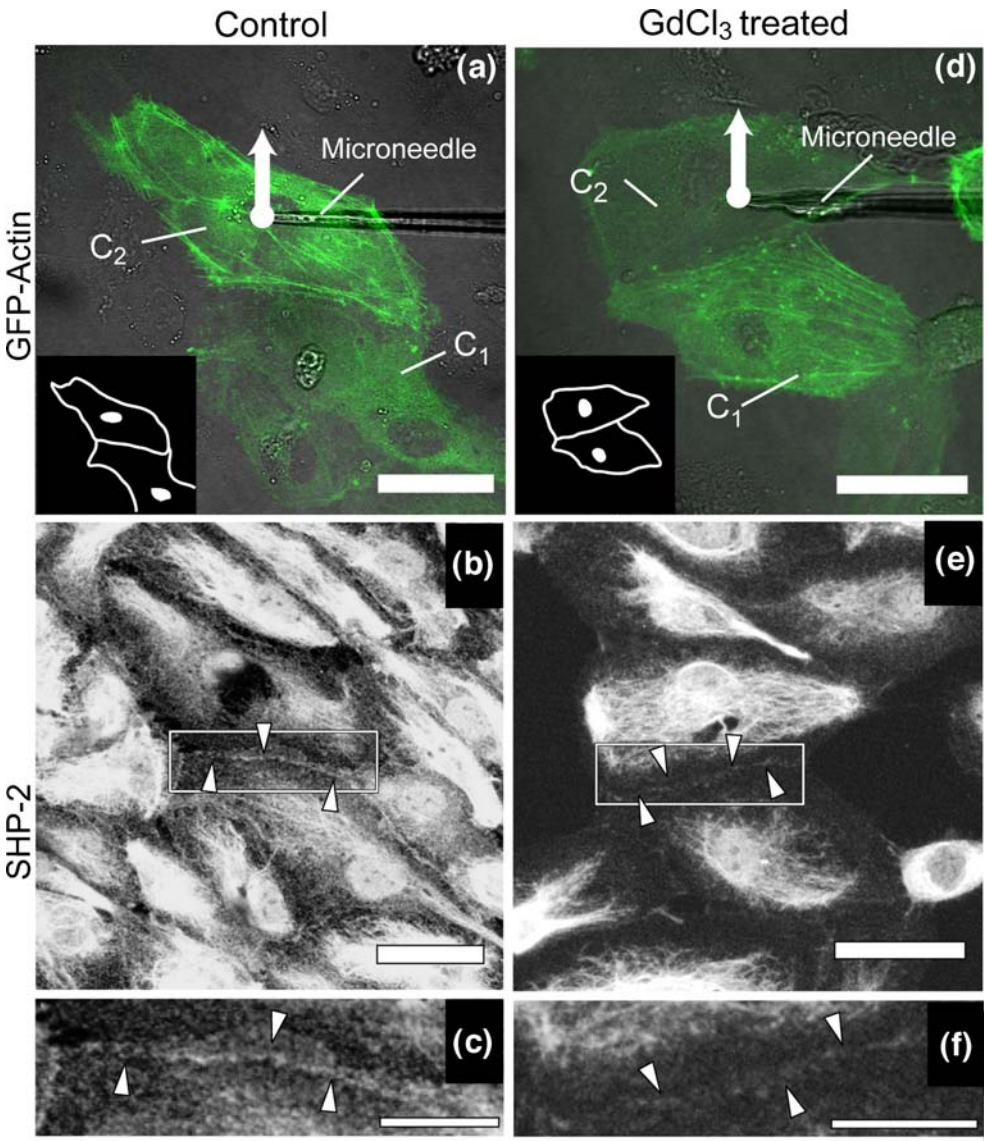

Fig. 6 Typical examples of fluorescent images of SHP-2 for control (**a**, **b**, **c**) and $GdCl_3$ treated ECs (**d**, **e**, **f**). Boxed regions in (**b**) and (**e**) are magnified in (**c**) and (**f**), respectively. Expression of SHP-2 was found to be localized at intercellular junctions (**b**, **d**; arrowheads). Bar=40 μm for (**a**, **b**, **d**, **e**), 20 μm for (**c**, **f**), respectively

these results and our results into consideration, there may exist specific time course of change depending on the type of externally applied mechanical stimuli. It is beyond our findings to see if the present remodeling process might be involved in the EC remodeling exposed to global mechanical stimuli including fluid shear stress. Figure 7 summarizes representative time course of EC remodeling process with GFP-actin together with schematic drawings representing cell morphology and actin organization. This result suggests that cell contraction or low angle of cell orientation should be prerequisite for EC elongation parallel to the direction of stretch. Noria et al. [20] suggested that flow-induced morphological changes of ECs were caused by reorganization of SFs. Moreover, Li et al. [21] reported that ECs transfected with dominant negative RhoA, responsible for SF formation, do not respond to fluid shear

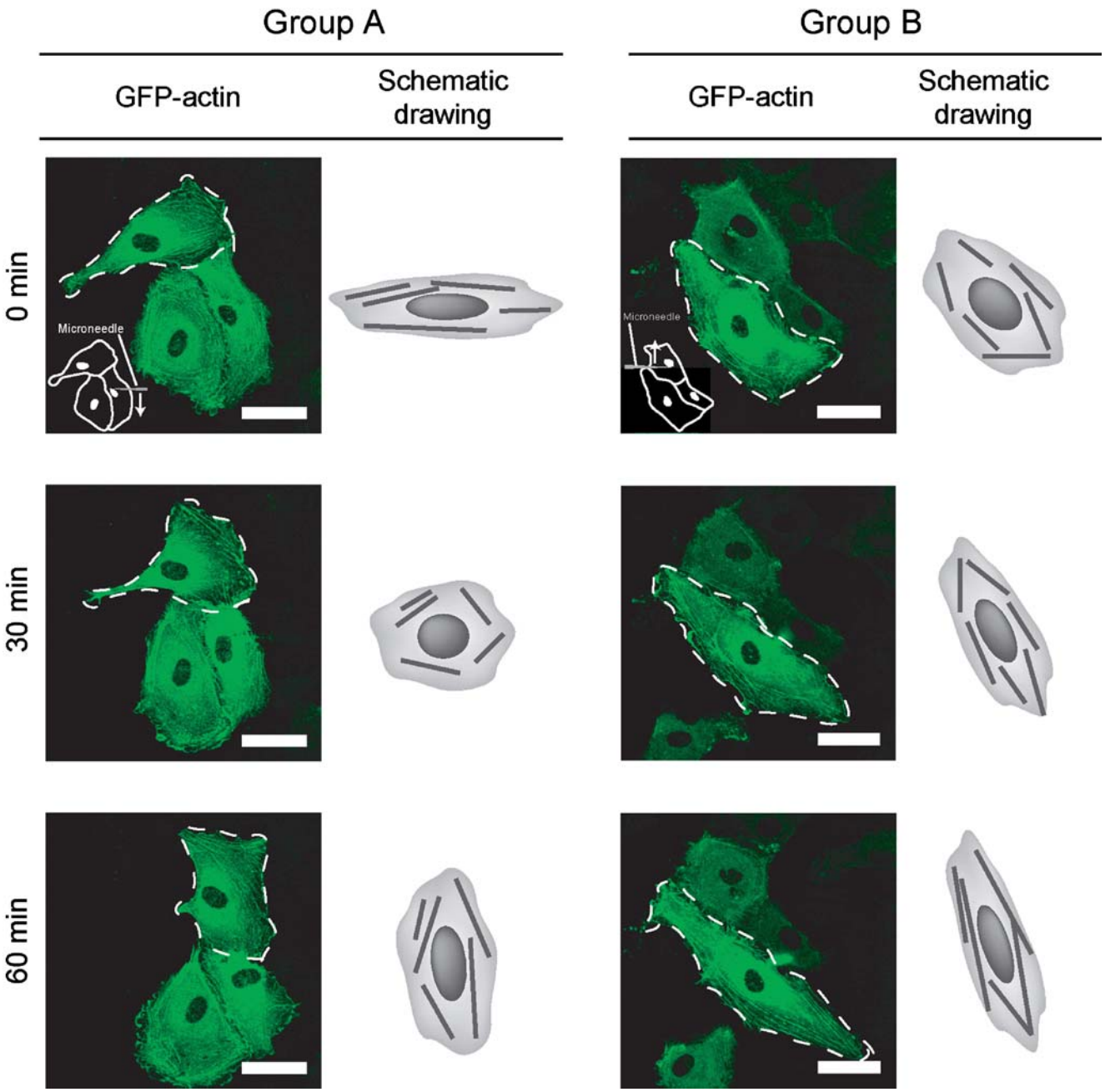

Fig. 7 Representative time course of EC remodeling process with fluorescent images and schematic drawings. Although time courses of change for the two groups are different, the observed ECs (C_1) finally elongated and orientated parallel to the direction of stretch

stress. Taken together, SF reorganization associated with cell morphological changes may play an important role in EC remodeling process.

Well-known mechanotransducers in EC remodeling to mechanical stimuli are SACs, integrins and PECAM-1. SACs are known to be activated by tension. Naruse et al. [22] reported that EC remodeling under exposure to cyclic stretch is inhibited by the blockade of SACs with $GdCl_3$ treatment. In this study, $GdCl_3$ treatment did not significantly affect either morphological changes or localization of SHP-2 at intercellular junctions, indicating that mechanotransduction of SACs does not have a pivotal role in the present EC remodeling. Osawa et al. [13] showed that when mechanotransduction by PECAM-1 occurred, SHP-2 molecules bound to phosphorylated PECAM-1 and recruited to cell-cell borders. Therefore, at least, mechanotransduction by PECAM-1 might be activated by application of local stretch in this study. A recent study [14] suggested that mechanotransduction by PECAM-1 may trigger flow-induced morphological changes of ECs. It is speculated that spatial gradient of magnitude of mechanical stimuli in cells might induce localized mechanotransduction by PECAM-1, possibly leading to the directional EC remodeling. To study this mechanism, further investigations in terms of the quantitative relationship between intracellular stress transfer and SHP-2/PECAM-1 expression should be included.

Conclusions

In this study, local stretch was applied to an EC to stimulate a neighboring EC via intercellular junctions using micromanipulation technique. ECs reorientated and elongated parallel to the direction of stretch. This remodeling process varied from cell to cell, particularly depending on initial cell shape. In addition, SHP-2 was found to be recruited to the stimulated intercellular junctions. These results strongly suggest that intercellular junctions can transmit mechanical forces between cells and transduce the forces into biochemical signals.

Acknowledgement The authors thank Dr. Ikuo Takahashi for kindly providing human umbilical cords. This work was in part supported financially by Grants-in-Aid for Scientific Research from the Ministry of Education, Culture, Sports, Science and Technology (MEXT) in Japan (Nos. 15086203, 17200030, 17680036).

Appendix. Calculation of SF parameters with image processing

The protocol for image processing to determine SF parameters is shown in Fig. 8. Algorithm based on pixel intensity of fluorescence images of GFP-actin was adapted from previous reports [23, 24]. SFs were extracted from original image [Fig. 8(a)] with convolution filter application, as shown in Fig. 8(b). For giving pixels $p_{i,j}$ in 8-bit gray-scale, the pixels surrounding $p_{i,j}$ were selected as a sample matrix [equation (1)]

$$\text{Sample matrix}(S_{i,j}) = \begin{pmatrix} p_{i-2,j-2} & p_{i-2,j-1} & p_{i-2,j} & p_{i-2,j+1} & p_{i-2,j+2} \\ p_{i-1,j-2} & p_{i-1,j-1} & p_{i-1,j} & p_{i-1,j+1} & p_{i-1,j+2} \\ p_{i,j-2} & p_{i,j-1} & p_{i,j} & p_{i,j+1} & p_{i,j+2} \\ p_{i+1,j-2} & p_{i+1,j-1} & p_{i+1,j} & p_{i+1,j+1} & p_{i+1,j+2} \\ p_{i+2,j-2} & p_{i+2,j-1} & p_{i+2,j} & p_{i+2,j+1} & p_{i+2,j+2} \end{pmatrix} \tag{1}$$

Convolution using horizontal and vertical kernels [equations (2) and (3)], which define weighted sum of neighboring pixels, provided magnitude of brightness gradient of SFs in each pixel [equation (4)].

$$\text{Vertical kernel } (K_{\text{v}}) = \begin{pmatrix} -1 & 0 & 2 & 0 & -1 \\ -2 & 0 & 4 & 0 & -2 \\ -4 & 0 & 8 & 0 & -4 \\ -2 & 0 & 4 & 0 & -2 \\ -1 & 0 & 2 & 0 & -1 \end{pmatrix} \tag{2}$$

$$\text{Horizonal kernel } (K_{\text{h}}) = K_v^T \tag{3}$$

$$G = S_{i,j} * K_{\text{h}} + S_{i,j} * K_{\text{v}} \tag{4}$$

The pixel whose G value was bigger than 5-fold of averaged pixel intensity in whole area of the target cell was assigned as a constituent of SFs. In order to calculate the angle of SF orientation, the angle of minimal gradient in pixel intensity in each pixel [Fig. 8(c)] was calculated using Sobel kernels as previously reported [20]. The angle data allocated to only pixels which have been assigned as a constituent of SFs [Fig. 8(d)]. Angle values were summed up across the cell with vectorial summation and were assumed that each pixel has a vector consisted of the calculated angle and unit length. The angle between the direction of the resultant vector and the tensile direction was defined as the angle of SF orientation. The length of the resultant vector divided by the number of pixels was defined as the uniformity index of SFs, which indicate the degree of alignment of SFs. All calculation processes were executed on Excel 2004 for Mac (Microsoft, USA). Analyses were performed on images obtained at every 5 min after application of local stretch.

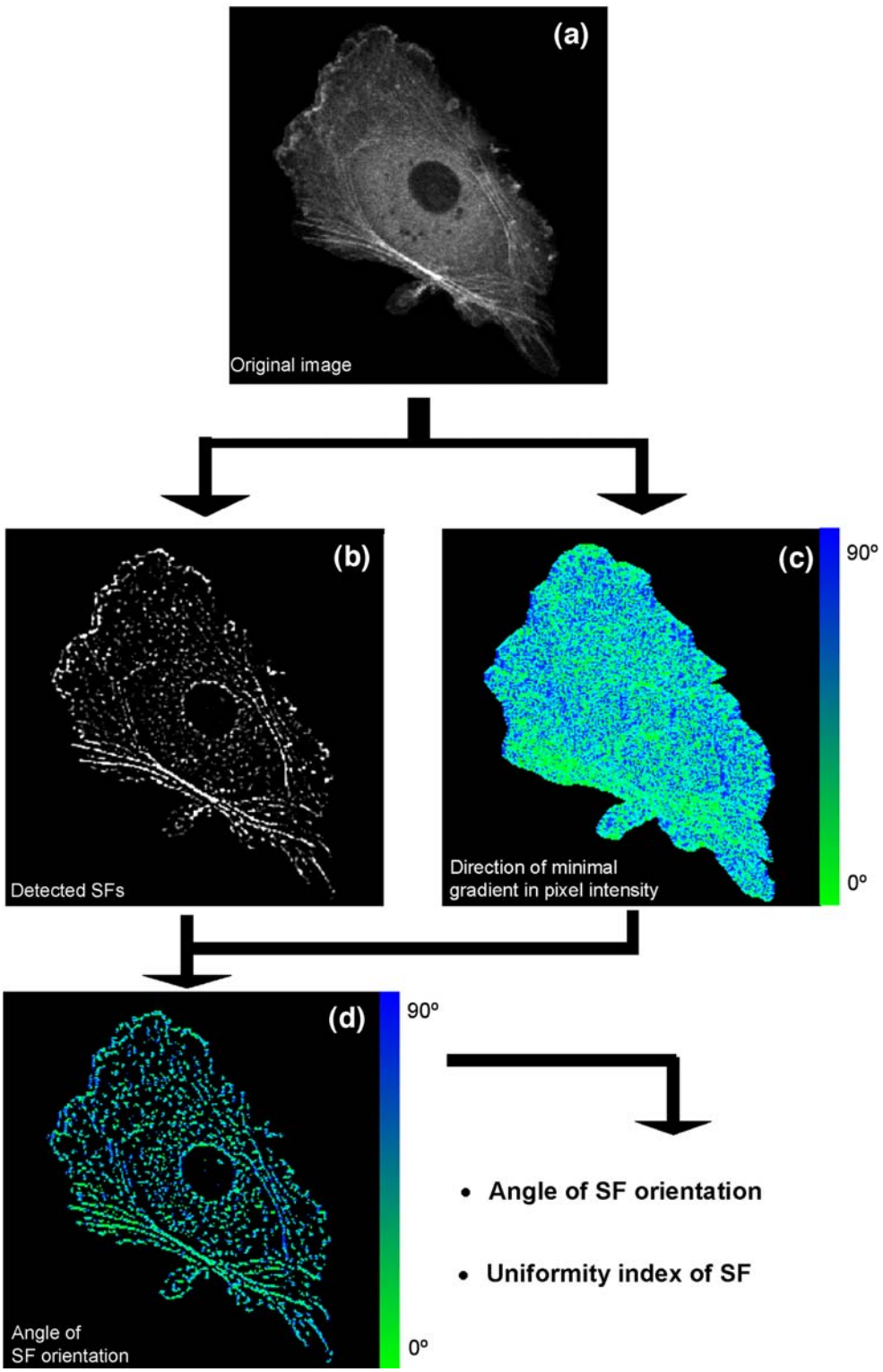

Fig. 8 Protocol for determination of SF parameters based on image processing. (**a**) Manually extracted single cell image, (**b**) automatically detected SFs with convolution filters, (**c**) calculated minimal gradient in pixel intensity with Sobel filter, (**d**) angle of SF orientation in each pixel

References

1. Dewey CF, Bussplari SR, Gimbrone MA, Davies PF (1981) The dynamic response of vascular endothelial cells to fluid shear stress. J Biomech Eng 103:177–185.
2. Galbraith CG, Skalak R, Chien S (1998) Shear stress induces spatial reorganization of the endothelial cell cytoskeleton. Cell Motil Cytoskelet 40:317–330.
3. Sato M, Nagayama K, Kataoka N, Sasaki M, Hane K (2000) Local mechanical properties measured by atomic force microscopy for cultured bovine endothelial cells exposed to shear stress. J Biomech 33:127–135.
4. Kataoka N, Ujita S, Sato M (1998) The effect of flow direction on the morphological responses of cultured bovine aortic endothelial cells. Med Biol Eng Comput 36:122–128.
5. Shirinsky VP, Antonov AS, Birukov KG, Sobolevsky AV, Romanov YA, Kabaeva NV, Antonova GN, Smirnov VN (1989) Mechano-chemical control of human endothelium orientation and size. J Cell Biol 109:331–339.
6. Wang JH, Goldschmidt-Clermont P, Wille J, Yin FC (2001) Specificity of endothelial cell reorientation in response to cyclic mechanical stretching. J Biomech 34:1563–1572.
7. Sugaya Y, Sakamoto N, Ohashi T, Sato M (2003) Elongation and random orientation of bovine endothelial cells in response to hydrostatic pressure: comparison with response to shear stress. JSME Int J Ser C 46:1248–1255.
8. Ohashi T, Sugaya Y, Sakamoto N, Sato M (2007) Hydrostatic pressure influences morphology and expression of VE-cadherin of vascular endothelial cells. J Biomech 40:2399–2405.
9. Albelda SM, Muller WA, Buck CA, Newman PJ (1991) Molecular and cellular properties of PECAM-1 (endoCAM/CD31): a novel vascular cell-cell adhesion molecule. J Cell Biol 114:1059–1068.
10. Ilan N, Cheung L, Pinter E, Madri JA (2000) Platelet-endothelial cell adhesion molecule-1 (CD31), a scaffolding molecule for selected catenin family members whose binding is mediated by different tyrosine and serine/threonine phosphorylation. J Biol Chem 275:21435–21443.
11. Kataoka N, Ujita S, Kimura K, Sato M (1998) The morphological responses of cultured bovine aortic endothelial cells to fluid-imposed shear stress sparse and colony conditions. JSME Int J Ser C 41:76–82.
12. Masuda M, Fujiwara K (1993) Morphological responses of single endothelial cells exposed to physiological levels of fluid shear stress. Front Med Biol Eng 5:79–87.
13. Osawa M, Masuda M, Kusano K, Fujiwara K (2002) Evidence for a role of platelet endothelial cell adhesion molecule-1 in endothelial cell mechanosignal transduction: is it a mechanoresponsive molecule? J Cell Biol 158:773–785.
14. Tzima E, Irani-Tehrani M, Kiosses WB, Dejana E, Schultz DA, Engelhardt B, Cao G, DeLisser H, Schwartz MA (2005) A mechanosensary complex that mediates the endothelial cell response to fluid shear stress. Nature 437:426–431.
15. Sakamoto N, Ohashi T, Sato M (2001) Effect of magnetic field on nitric oxide synthesis of cultured endothelial cells. Int J Appl Electromagn Mech 14:317–322.
16. Sokabe M, Hayakawa K, Tatsumi H (2005) Varieties of mechanotransduction: the cytoskeletal stress fibre as a force transmitter and a mechanosensor. Proc Aust Physiol Soc 36:95.
17. Sasamoto A, Nagino M, Kobayashi S, Naruse K, Nimura Y, Sokabe M (2005) Mechanotransduction by integrin is essential for IL-6 secretion from endothelial cells in response to uniaxial continuous stretch. Am J Physiol, Cell Physiol 288:C1012–1022.
18. Ohashi T, Sugawara H, Matsumoto T, Sato M (2000) Surface topography measurement and intracellular stress analysis of cultured endothelial cells exposed to fluid shear stress. JSME Int J Ser C 43:780–786.
19. Tzima E, Del Pozo MA, Kiosses WB, Mohamed SA, Li S, Chien S, Schwartz MA (2002) Activation of Rac1 by shear stress in endothelial cells mediates both cytoskeletal reorganization and effects on gene expression. EMBO J 21:6791–6800.
20. Noria S, Xu F, McCue S, Jones M, Gotlieb AI, Langille BL (2004) Assembly and reorientation of stress fibers drives morphological changes to endothelial cells exposed to shear stress. Am J Pathol 164:1211–1223.
21. Li S, Chen BP, Azuma N, Hu YL, Wu SZ, Sumpio BE, Shyy JY, Chien S (1999) Distinct roles for the small GTPases Cdc42 and Rho in endothelial responses to shear stress. J Clin Invest 103:1141–1150.
22. Naruse K, Yamada T, Sokabe M (1998) Involvement of SA channels in orienting response of cultured endothelial cells to cyclic stretch. Am J Physiol 274:H1532–1538.
23. Yoshigi M, Clark EB, Yost HJ (2003) Quantification of stretch-induced cytoskeletal remodeling in vascular endothelial cells by image processing. Cytometry A 55:109–118.
24. Kaunas R, Nguyen P, Usami S, Chien S (2005) Cooperative effects of Rho and mechanical stretch on stress fiber organization. Proc Natl Acad Sci 102:15895–15900.